Cytotechnology (2010) 62:519–529
DOI 10.1007/s10616-010-9313-x

METHOD IN CELL SCIENCE

Characterization and use of human brain microvascular endothelial cells to examine β-amyloid exchange in the blood-brain barrier

Corbin Bachmeier · Michael Mullan · Daniel Paris

Received: 30 August 2010 / Accepted: 3 October 2010 / Published online: 19 October 2010

Abstract Alzheimer's disease (AD) is characterized by excessive cerebrovascular deposition of the β-amyloid peptide (Aβ). The investigation of Aβ transport across the blood-brain barrier (BBB) has been hindered by inherent limitations in the cellular systems currently used to model the BBB, such as insufficient barrier properties and poor reproducibility. In addition, many of the existing models are not of human or brain origin and are often arduous to establish and maintain. Thus, we characterized an in vitro model of the BBB employing human brain microvascular endothelial cells (HBMEC) and evaluated its utility to investigate Aβ exchange at the blood-brain interface. Our HBMEC model offers an ease of culture compared with primary isolated or coculture BBB models and is more representative of the human brain endothelium than many of the cell lines currently used to study the BBB. In our studies, the HBMEC model exhibited barrier properties comparable to existing BBB models as evidenced by the restricted permeability of a known paracellular marker. In addition, using a simple and rapid fluormetric assay, we showed that antagonism of key Aβ transport proteins significantly altered the bi-directional transcytosis of fluorescein-Aβ (1–42) across the HBMEC model. Moreover, the magnitude of these effects was consistent with reports in the literature using the same ligands in existing in vitro models of the BBB. These studies establish the HBMEC as a representative in vitro model of the BBB and offer a rapid fluorometric method of assessing Aβ exchange between the periphery and the brain.

Keywords Alzheimer's disease · Blood-brain barrier · Beta-amyloid · LRP1 · RAGE

C. Bachmeier (✉) · M. Mullan · D. Paris
The Roskamp Institute, 2040 Whitfield Avenue, Sarasota, FL 34243, USA
e-mail: cbachmeier@rfdn.org

Introduction

Alzheimer's disease (AD) is a neurodegenerative process resulting in neuronal cell loss, cognitive decline and ultimately, death. The pathology of AD is characterized by the formation of intra-neuronal fibrillary tangles and the deposition of beta-amyloid protein (Aβ) in the brain and cerebrovasculature (Mehta 2007). Aβ accumulation in the brain appears to be a key factor in AD pathology as the appearance of soluble Aβ precedes the neuroinflammatory and neurotoxic events associated with this disease (LaFerla et al. 2007; Lue et al. 1999). A thorough understanding of the mechanisms controlling Aβ levels in the brain is necessary in developing effective strategies for the treatment of AD. The system responsible for managing Aβ exchange between the brain and the blood is the blood-brain barrier (BBB) (Engelhardt and Sorokin 2009). The BBB plays a vital role in attenuating the

concentrations of Aβ exposed to the brain and a loss of BBB function may lead to abnormal deposition of Aβ in the cerebrovasculature (e.g., cerebral amyloid angiopathy) and/or excessive Aβ accumulation in the brain parenchyma (e.g., AD). The development of a representative in vitro model of the BBB is critical in advancing our understanding of Aβ's contribution to disease pathology.

A variety of cellular systems have been used to represent the BBB including those comprised of primary cultures, co-cultures, and cell lines, each of which have inherent advantages and disadvantages (for a complete review of the cellular systems used as in vitro models of the BBB and the factors that influence BBB permeability, see Deli et al., 2005). While the primary culture and co-culture systems most closely resemble the BBB in vivo, development of these models is generally a labor intensive process that requires significant time and technical resources (Deli et al. 2005; Eddy et al. 1997). In addition, these systems are often fraught with poor reproducibility and, since nearly all of them utilize non-human tissue, these models may not be fully representative of the human BBB (Gumbleton and Audus 2001). Another cellular system used to model the BBB incorporates the use of immortalized cell lines. Unlike the primary or co-culture models, these cells can be established rapidly, are easily maintained, and offer a relatively reproducible phenotype (Terasaki and Hosoya 2001). However, many of the cell lines currently employed are derived from tissues that are not of brain origin and therefore lack cerebral-specific markers. In recent years there has been a concerted effort to develop an immortalized brain endothelial cell line and, as a result, numerous lines of various species origin have been generated (Deli et al. 2005). While these lines have been useful in addressing questions related to cerebrovascular pathophysiology or cell biology, they universally fail to generate sufficiently restrictive barrier properties (Gumbleton and Audus 2001).

The limitations associated with existing in vitro models of the BBB have stifled our ability to investigate Aβ exchange between the periphery and the brain. In this report we present an in vitro BBB model of human brain origin that demonstrates restrictive barrier properties and is easily maintained. Additionally, we characterized the ability of this model to investigate Aβ-related transport phenomena at the blood-brain interface. In doing so, we established a simple and rapid fluorometric method of evaluating Aβ exchange in the BBB using a human in vitro model.

Materials

Human brain microvascular endothelial cells (HBMEC), endothelial cell medium (ECM), endothelial cell growth supplement (ECGS), human astrocytes (HA), astrocyte medium (AM), astrocyte growth supplement (AGS), fetal bovine serum, and penicillin/streptomycin solution, was purchased from Sciencell Research Laboratories (Carlsbad, CA). Fibronectin solution and 4kD Fluorescein isothiocyanate–dextran (FD4) were purchased from Sigma Chemical Co. (St. Louis, MO). Fluorescein-Aβ (1–42) was purchased from rPeptide (Bogart, GA). Unlabeled human Aβ (1–42) was purchased from Invitrogen Corp. (Carlsbad, CA). Human recombinant apolipoprotein E (isoform E3), human recombinant receptor associated protein (RAP), and mouse monoclonal low density lipoprotein receptor-related protein 1 (LRP1) antibody (8G1) were purchased from EMD Chemicals Inc. (Hawthorne, NY). Human recombinant high mobility group box 1 protein (HMGB1) and a mouse monoclonal anti-human receptor for advanced glycation end products (RAGE) antibody were purchased from R&D Systems (Minneapolis, MN). The rabbit polyclonal RAGE antibody was purchased from Santa Cruz Biotechnology, Inc. (Santa Cruz, CA). The 24-well membrane inserts (translucent, 0.4 μm pore), 24-well companion plates, and 6-well plates were purchased from Fisher Scientific (St. Louis, MO).

Methods

Cell culturing

HBMEC were seeded at 50,000 cells/cm^2 onto fibronectin-coated (4 μg/cm^2), 24-well, 0.4 μm-pore, translucent membrane inserts (0.3 cm^2/insert) to establish a polarized monolayer representative of the BBB. The layer of endothelial cells separates this system into an apical ("blood" side) and basolateral ("brain" side) compartment. This setup provides a mechanism for administering or sampling compounds on either side of the BBB model. The culture medium

(ECM) was supplemented with 5% fetal bovine serum, 1% penicillin/streptomycin solution, and 1% growth supplement (ECGS). For the co-culture model, HA were seeded at 50,000 cells/cm^2 into the wells of the 24-well carrier plates (1.9 cm^2/well). The culture medium (AM) was supplemented with 5% fetal bovine serum, 1% penicillin/streptomycin solution, and 1% growth supplement (AGS). All cells were cultured in a humidified 37 °C incubator with 5% CO_2. Medium replacement was carried out every other day until the monolayers reached confluence (3–4 days). HA-conditioned medium was collected from confluent HA monolayers over a period of 4 days.

Peptide preparation

Using a standard process to limit aggregation, Aβ peptides were solubilized in 1,1,1,3,3,3-hexafluoro-2-propanol (HFIP) to acquire a monomeric sample and minimize the formation of β-sheet structures. Briefly, 1 mg of each lyophilized peptide was dissolved in 1 mL of HFIP. The peptides were allowed to air dry in a chemical fume hood for 1 h followed by further drying in a speed-vac centrifuge for 30 min. The resulting clear film was re-suspended in 100% dimethylsulfoxide (DMSO) to a concentration of 1 mM and stored at −80 °C.

In vitro BBB model

To establish an in vitro co-culture model of the BBB, HBMEC and HA were cultured as described above. 24 h after seeding, for a period of 3–4 days, the HBMEC-cultured inserts were either bathed in HA-conditioned medium or placed in contact with blank medium in the wells of a 24-well plate that contained growing HA cells. This coculture represents a noncontact model where there is no cell to cell contact between the HBMEC (on the inserts) and the HA (on the surface of the wells). Following the 3–4 day exposure, all medium was removed and the inserts were relocated to new wells for experimentation. In addition, a cell-free fibronectin-coated group of inserts was prepared. ECM containing 10 μM FD4 was placed in the basolateral (donor) compartment of each group while the apical (receiver) side of the membrane was exposed to medium alone. The donor compartment was sampled at time 0 to establish the initial concentration of FD4 in each group. Following exposure of the inserts to the wells containing FD4, the plate was incubated at 37 °C. Samples were collected from the apical compartment at various time points up to 120 min to assess the movement of FD4 across the HBMEC monolayer (basolateral to apical). The samples were analyzed (λex = 485 nm and λem = 516 nm) for FD4 using a BioTek Synergy HT multi-detection microplate reader (Winooski, VT). The apparent permeability (Papp) of FD4 was determined using the equation Papp = $1/AC_0$ * (dQ/dt), where A represents the surface area of the membrane, C_0 is the initial concentration of FD4 in the basolateral compartment, and dQ/dt is the amount of FD4 that appears in the apical compartment in the given time period (Artursson 1990).

Impact of Aβ on HBMEC integrity

Using the same methodology described above, ECM containing 10 μM FD4 was placed in the basolateral compartment of the in vitro BBB model consisting of a confluent HBMEC monolayer grown on 24-well inserts in the absence of HA. For these studies, the apical side of the membrane was exposed to various concentrations (0.5, 1, and 2 μM) of unlabeled Aβ (1–42). Samples were collected and analyzed for FD4 content in the same manner described above. The Papp of FD4 in the presence of Aβ was compared to control (i.e., no Aβ exposure) and expressed as a percentage.

Permeability of FD4 versus fluorescein-Aβ (1–42)

These studies were performed using a methodology similar to that established above. Briefly, the basolateral compartment of the in vitro BBB model was exposed to 10 μM FD4 or 2 μM fluorescein-Aβ (1–42) while the apical side of the membrane contained ECM only. The apical compartment was sampled at 30 and 60 min for the appearance of FD4 or fluorescein-Aβ (1–42) and analyzed using the parameters described above.

Expression and function of Aβ transporters in HBMEC

Expression

To evaluate the expression of LRP1 and RAGE, HBMEC were seeded at 100,000 cells/cm^2 onto

fibronectin-coated (1 μg/cm^2), 6-well (9.6 cm^2/well) plates. The endothelial cell culture medium (ECM) was supplemented with 5% fetal bovine serum, 1% penicillin/streptomycin solution, and 1% endothelial cell growth supplement. The cells were cultured in a humidified 37 °C incubator with 5% CO_2. Medium replacement was carried out every other day until the monolayers reached confluence (3–4 days). Upon confluency, monolayers were washed with PBS and each well exposed to 150μL of ice-cold M-PER reagent (Pierce Biotechnology, Rockford, IL) containing phenylmethanesulfonyl fluoride (1 mM) and Halt Protease and Phosphatase Inhibitor Cocktail (1X) (Thermo Scientific, Waltham, MA). Samples were placed at −80 °C until collection. Cell lysates from each group were collected and evaluated for protein content using the bicinchoninic acid (BCA) method (Thermo Scientific, Waltham, MA). Samples were denatured by boiling in Laemmli Buffer (Bio-Rad, Hercules, CA) and loaded (50 μg of protein) onto a Criterion 4–20% Tris-HCl gradient gel (Bio-Rad, Hercules, CA). Migration transpired using 50–130 V over a 2 h period. Following migration, electrotransfer to an Immun-Blot PVDF (polyvinylidene fluoride) membrane occurred overnight at 4 °C and 90 mA. The membrane was immunoprobed with mouse monoclonal LRP1 antibody (1:5,000 dilution) or rabbit polyclonal RAGE antibody (1:1,000 dilution) in 5% Blotting-Grade Blocker (nonfat dry milk) (Bio-Rad, Hercules, CA) for 3 h. The membrane was washed with deionized water and exposed to HRP-linked mouse secondary antibody (Cell Signaling Technology, Inc., Danvers, MA) for 1 h. Following a 30 min wash in deionized water, the membrane was revealed using SuperSignal West Femto Maximum Sensitivity Substrate (Thermo Scientific, Waltham, MA) and exposed with a Bio-Rad ChemiDoc XRS molecular imager (Bio-Rad, Hercules, CA).

Function

These studies were performed using the permeability methodology described earlier. Again, 2 μM fluorescein-Aβ (1–42) was placed in the basolateral compartment. For the studies evaluating LRP1 activity, the LRP1 ligands RAP (200 nM) or apoE (25–400 nM) were added to the basolateral compartment. As above, samples were collected from the apical compartment for the detection of fluorescein-Aβ (1–42). To examine RAGE interactions, 2 μM fluorescein-Aβ (1–42) was placed in either the apical or basolateral compartments. At the same time, various concentrations (4, 10, and 40 μg/mL) of a mouse monoclonal RAGE blocking antibody were exposed to the apical side of the membrane. The side of the membrane opposing the fluorescent probe was sampled at 30 and 60 min to quantitate the presence of fluorescein-Aβ (1–42). In a similar study, the impact of a known ligand of RAGE, HMGB1 (0.1 to 5 μg/mL), was examined following exposure to the apical compartment. The amount of fluorescein-Aβ (1–42) navigating across the HBMEC under these conditions was calculated as described earlier and expressed as a percentage of control.

Statistics

Statistical analyses were performed using an ANOVA and the Student-Newman-Keuls multiple comparisons post-hoc test. The half maximal inhibitory concentration (IC_{50}) was determined using GraphPad Prism 5 (GraphPad Software, Inc., La Jolla, CA).

Results

In vitro BBB models

The movement of the paracellular marker, FD4, across a membrane constituting various in vitro models of the BBB is displayed in Fig. 1a. Each of the cellular BBB models presented a significant obstacle to the permeability of FD4 across the membrane. The amount of FD4 that crossed the various cellular models over 120 min was approximately 6 times less than that observed under cell-free conditions. Exposure of the HBMEC to astrocytes or astrocyte conditioned medium did not influence FD4 permeability as no difference was observed between the various cellular conditions (Fig. 1a). The apparent permeability (Papp) of FD4 was 30.9×10^{-6} cm/s in the cell free assay compared to an average of 5.5×10^{-6} cm/s for the cellular BBB models.

Impact of Aβ on HBMEC integrity

To assess the influence of Aβ (1–42) on the paracellular integrity of the HBMEC model, the permeability of FD4 in the presence of various

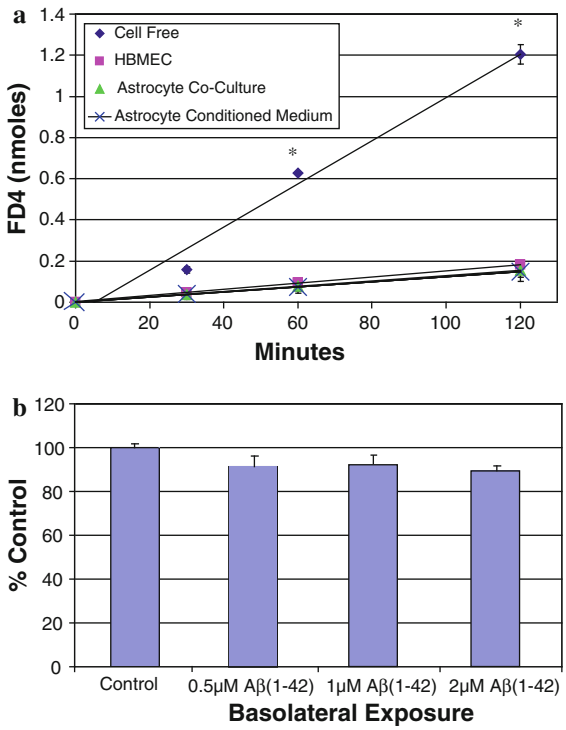

Fig. 1 Basolateral-to-apical movement of FD4 (**a**) under cell free conditions and across various in vitro models of the BBB and (**b**) in the presence of unlabeled Aβ (1–42) exposed to the basolateral compartment of the HBMEC model. In each scenario, 10 μM FD4 was placed in the basolateral compartment and samples were collected from the apical compartment over a period of 120 min. Values represent mean ± SEM (n = 3). * $p < 0.05$ for cell free conditions compared to each in vitro BBB model as determined by ANOVA and the Student-Newman-Keuls multiple comparisons post-hoc test. Comparisons between the in vitro BBB models were not significant at any time point. None of the groups exposed to unlabeled Aβ (1–42) reached statistical significance when compared to control

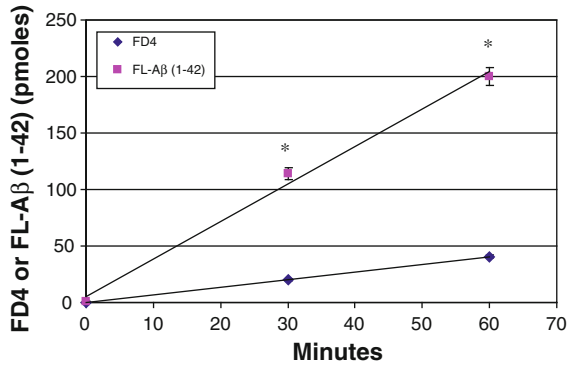

Fig. 2 Basolateral-to-apical movement of FD4 or fluorescein-Aβ (1–42) across the HBMEC model. 10 μM FD4 or 2 μM fluorescein-Aβ (1–42) was placed in the basolateral compartment and samples were collected from the apical compartment at 30 and 60 min to assess the amount of each probe traversing the cell monolayer. Values represent mean ± SEM (n = 3). * $p < 0.05$ for fluorescein-Aβ (1–42) compared to FD4 as determined by ANOVA and the Student-Newman-Keuls multiple comparisons post-hoc test

concentrations of Aβ was evaluated in the HBMEC and is presented in Fig. 1b. The permeability of the HBMEC to FD4 was not significantly altered by the presence of Aβ (1–42) at any of the concentrations examined.

Permeability of FD4 versus fluorescein-Aβ (1–42)

A comparison of the permeabilities of FD4 and fluorescein-Aβ (1–42) across the HBMEC over time is represented in Fig. 2. The basolateral-to-apical movement of fluorescein-Aβ (1–42) was 5 times greater than FD4 at 60 min (Fig. 2). This translates to a >10-fold difference in Papp (56.1×10^{-6} cm/s for fluorescein-Aβ (1–42) versus 4.6×10^{-6} cm/s for FD4). We also performed identical studies using unlabeled Aβ (1–42) and an enzyme-linked immunosorbent assay (ELISA) for human Aβ (1–42) as the method of detection (Invitrogen Corp., Carlsbad, CA). The basolateral-to-apical permeability of unlabeled Aβ (1–42) was similar to that observed with fluorescein-Aβ (1–42) across the HBMEC model, indicating the fluorescein label does not alter the cellular transcytosis of Aβ (data not shown).

Expression and function of Aβ transporters in HBMEC

Figure 3 reveals the expression of RAGE (46 kDa) and LRP1 (515 kDa) in the HBMEC. Figure 4 illustrates the effect of known LRP1 ligands on fluorescein-Aβ (1–42) transcytosis across the HBMEC. Exposure of RAP to the basolateral side of the BBB model dramatically influenced the basolateral-to-apical clearance of fluorescein-Aβ (1–42), reducing the appearance of the probe in the apical compartment by 70% (Fig. 4a). Similarly, basolateral administration of ApoE3 also inhibited the removal of fluorescein-Aβ (1–42) from the basolateral compartment in a dose-dependent manner (Fig. 4b). The highest concentration of ApoE3 examined (400 nM) reduced the

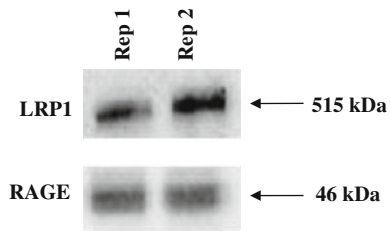

Fig. 3 Representative immunoblots of LRP1 and RAGE in the HBMEC

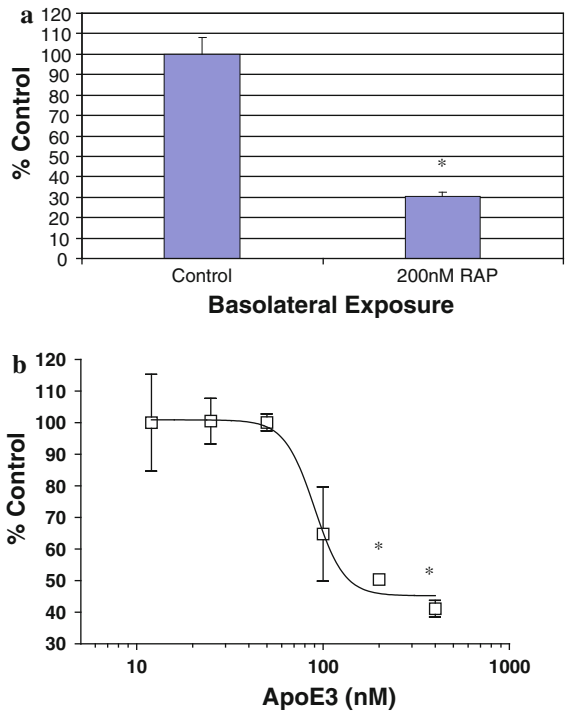

Fig. 4 Basolateral-to-apical transcytosis of fluorescein-Aβ (1–42) across the HBMEC model in the presence of (**a**) RAP or (**b**) ApoE3. Both fluorescein-Aβ (1–42) (2 μM) and a LRP1 ligand was exposed to the basolateral compartment of the HBMEC model. Samples were collected from the apical compartment at 30 and 60 min to examine fluorescein-Aβ (1–42) transcytosis across the cell monolayer. The apparent permeability of fluorescein-Aβ (1–42) in the presence of each LRP1 ligand was determined and expressed as a percentage of control. Values represent mean ± SEM (n = 3). * $p < 0.05$ as determined by ANOVA and the Student-Newman-Keuls multiple comparisons post-hoc test

movement of fluorescein-Aβ (1–42) by half. Using a nonlinear dose-response regression of the curve, the IC_{50} calculated for this interaction was 89.9nM.

In a similar manner, a known RAGE ligand, HMGB1, and an antibody for RAGE were investigated for their impact on fluorescein-Aβ (1–42) transcytosis across the HBMEC, the results of which are presented in Fig. 5. Exposure of HMGB1 or a RAGE antibody to the apical compartment of the BBB model significantly enhanced the basolateral-to-apical clearance of fluorescein-Aβ (1–42) across the HBMEC. At 5 μg/mL, HMGB1 increased fluorescein-Aβ (1–42) transcytosis by 75% (Fig. 5a), while 40 μg/mL of a RAGE antibody produced similar results (Fig. 5b). Consistently, co-administration of fluorescein-Aβ (1–42) and RAGE antibody to the apical side of the HBMEC membrane resulted in a significant decrease in the transcytosis of fluorescein-Aβ (1–42) into the basolateral compartment. A 40% reduction in the movement of fluorescein-Aβ (1–42) was observed in the presence of 10 μg/mL of RAGE antibody (Fig. 5c).

Discussion

The purpose of these studies was to characterize a primary human brain endothelial cell (HBMEC) model as an in vitro representation of the BBB. In addition, we evaluated the suitability of this model to investigate Aβ exchange at the blood-brain interface and, in the process, established a rapid fluorometic method of examining Aβ transport dynamics in the BBB. As described earlier, a number of cellular models have been used to mimic the BBB including primary cells, co-cultures, and cell lines. As our model is derived from human brain tissue it expresses a phenotype that is more representative of the BBB in vivo than cell lines originating from other species or non-cerebral tissue. At the same time, these cells adorn the simplicity and ease of use of immortalized cultures.

Many of the current in vitro BBB models utilize a co-culture strategy, the most prevalent of which incorporates astrocytes or astrocyte-conditioned medium. In our studies, exposure of astrocyte co-culture conditions to the HBMEC did not significantly enhance the junctional resistance of this BBB model. While numerous studies exploring the use of brain endothelial cells as a model for the BBB have demonstrated improvements in "barrier" properties through the application of a co-culture system, many studies were unable to observe demonstrable benefits. For example, using similar conditions and methodology as the current study, Guerin and Bobilya

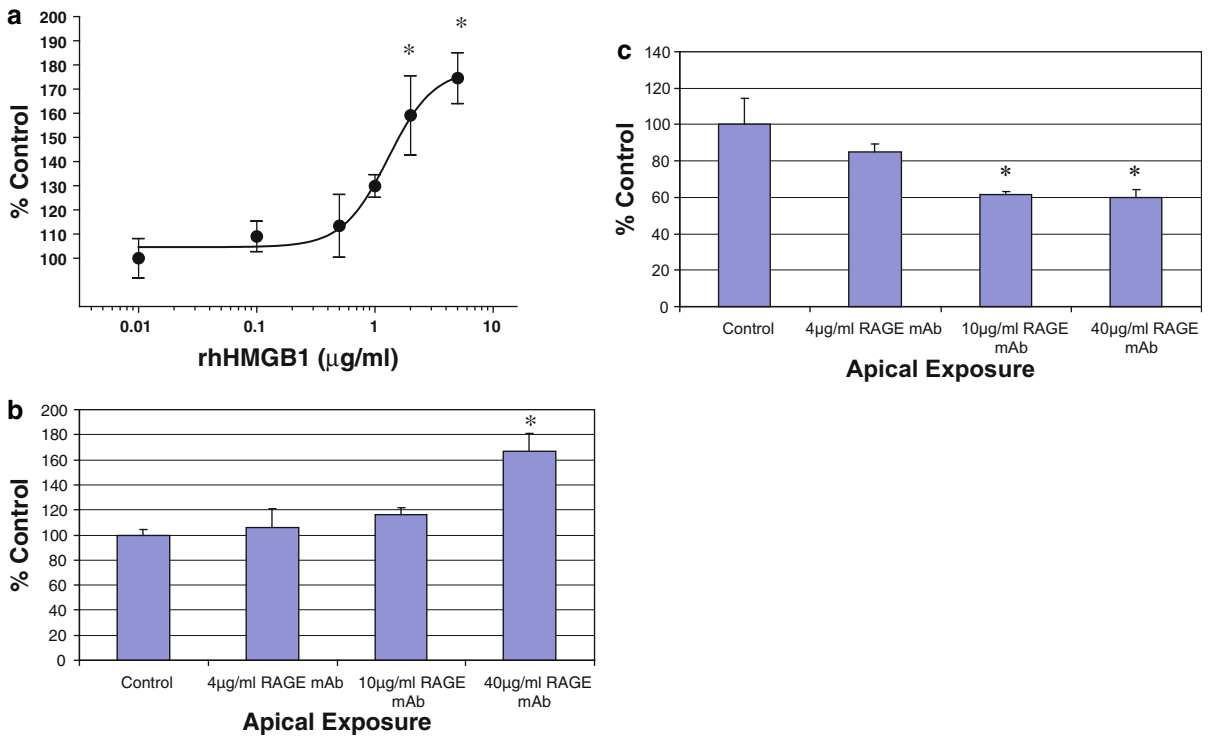

Fig. 5 Cellular transcytosis of fluorescein-Aβ (1–42) across the HBMEC model in the presence of (**a**) rhHMGB1 or (**b**) a RAGE monoclonal antibody (mAb). Fluorescein-Aβ (1–42) (2 μM) was exposed to the basolateral compartment of the HBMEC model while rhHMGB1 or a RAGE mAb was exposed to the apical compartment. Samples were collected from the apical compartment at 30 and 60 min to examine fluorescein-Aβ (1–42) transcytosis across the cell monolayer (basolateral-to-apical). For (**c**), both fluorescein-Aβ (1–42) (2 μM) and a RAGE mAb were exposed to the apical compartment of the HBMEC model. Samples were collected from the basolateral compartment at 30 and 60 min to examine fluorescein-Aβ (1–42) transcytosis across the cell monolayer (apical-to-basolateral). The apparent permeability of fluorescein-Aβ (1–42) under each treatment condition was determined and expressed as a percentage of control. Values represent mean ± SEM (n = 3–9). * $p < 0.05$ as determined by an ANOVA and the Student-Newman-Keuls multiple comparisons post-hoc test

investigated the impact of noncontact co-culture conditions on the integrity of a porcine brain capillary endothelial cell (PBCEC) model (Guerin and Bobilya 1997). Based on their resistance to the passage of macromolecules and small ions, PBCECs co-cultured with astrocytes or exposed to astrocyte-conditioned medium did not enhance the integrity of the porcine BBB model (Guerin and Bobilya 1997). As this observation and the current study employed a non-contact coculture model, it should be noted that direct contact or mixed co-cultures do not necessarily improve in vitro BBB resistance either. Ma et al. examined numerous co-culture models consisting of brain endothelial cells (rat and bovine) and rat astrocytes. As determined by the transendothelial electrical resistances (TEER, a measure of barrier tightness) of each endothelial and astrocyte co-culture model, the results indicated a lack of synergy between the two cell types in forming a tighter barrier (Ma et al. 2005). Using commercially available brain endothelial cells, like the current model, a recent study observed no difference between monoculture and astrocyte co-culture models in the diffuse permeability of three solutes (Li et al. 2010). More notably, there was no significant difference in the permeability of 70 kDa dextran in the endothelial monoculture model compared with in vivo data from rat cerebral microvessels, demonstrating the resemblance of such BBB models, like the current HBMEC model, to conditions in a live animal (Li et al. 2010).

Regardless of the culture conditions, the overarching goal is to identify a BBB model that exhibits restrictive barrier properties. The HBMEC model in the current study presented a significant obstacle to

the movement of the well established, paracellular marker, FD4 (4kD), as evidenced by the comparison to cell free conditions. The magnitude of this difference is similar to that reported for a molecule of the same molecular weight in a bovine model of the BBB (Strazielle et al. 2000). In this paper, the clearance of 4kD polyethylene glycol (PEG) was 10-fold greater in cell free inserts compared to those grown with the bovine brain endothelial cells, an observation similar to that demonstrated for FD4 in the HBMEC in the present study. Most notably, Gaillard and de Boer examined the permeability profile of FD4 using an established in vitro BBB model comprising brain capillary endothelial cells (BCEC) and astrocytes co-cultured on semi-permeable filter inserts. The range of the basal apparent permeability values reported for FD4 in this co-culture BBB model was 0.3–7.3 $\times$ 10^{-6} cm/s (Gaillard and de Boer 2000). The average basal apparent permeability of FD4 in the HBMEC model from the current study falls within this range (5.2 $\times$ 10^{-6} cm/s). Although the in vitro BBB model examined in the current study does not utilize a co-culture mechanism, these examples indicate the HBMEC model imparts a substantial barrier to paracellular movement that is comparable to existing BBB models.

Numerous structural and functional cerebromicrovasular abnormalities have been associated with AD. One of the pathological consequences of AD is a progressive loss of BBB function that has been described in patients with AD (Bowman et al. 2007; Skoog et al. 1998; Zipser et al. 2007), animal models of AD (Jancso et al. 1998; Ujiie et al. 2003), and in cell culture experiments (Gonzalez-Velasquez et al. 2008; Marco and Skaper 2006; Strazielle et al. 2000). It is now well accepted that the altered BBB permeability in AD is due, in part, to the presence of Aβ as determined through both in vitro (Gonzalez-Velasquez et al. 2008; Marco and Skaper 2006; Strazielle et al. 2000) and in vivo (Jancso et al. 1998; Ujiie et al. 2003) observations. As we are interested in using the HBMEC model to investigate Aβ exchange dymanics in the BBB, it is essential that Aβ itself does not compromise the integrity of the BBB model. We did not observe changes in FD4 permeability in the HBMEC model following exposure of up to 2 μM Aβ (1–42). This is likely due to both the form (soluble) and concentration of Aβ we exposed to the HBMEC. Using the same in vitro BBB model as the current study (human brain microvascular endothelial monolayers), Gonzalez-Velasquez and colleagues observed Aβ(1–40)-induced changes in permeability and TEER, in addition to a re-localization of the tight junction-associated protein zonula occludin-1 away from cell borders and into the cytoplasm (Gonzalez-Velasquez et al. 2008). However, these effects were only apparent with Aβ aggregates and not the unaggregated monomeric form (Gonzalez-Velasquez et al. 2008). A recent study reported similar findings for Aβ (1–42). It was determined that Aβ (1–42) fibrils, but not monomers, were found to increase the permeability of the endothelium in a dose- and time-dependent manner as detected by induced changes in the cytoskeletal network (Nagababu et al. 2009). All of our studies used monomeric/dimeric Aβ, solubilized via a standard process to limit aggregation (Giliberto et al. 2008). Another aspect to consider is the concentration of Aβ that is exposed to the cell monolayer. Our studies used 2 μM Aβ (1–42), mostly exposing Aβ to the basloateral side of the endothelium. This concentration appears to be well below the levels required to alter BBB permeability. For instance, Strazielle et al. did see a doubling in the flux of a paracellular tracer, polyethylene glycol (PEG), across the BBB following the introduction of soluble Aβ (1–40), but that only occurred when the apical concentration was raised to 5 μM (Strazielle et al. 2000). In addition, it took over 2 h to observe this same effect following exposure of 5 μM to the basolateral side. The flux of PEG was unaltered in the presence of Aβ concentrations below 5 μM, regardless of Aβ's orientation (Strazielle et al. 2000). All of our studies were performed in less than 2 h using an Aβ concentration of 2 μM. Exposure to Aβ (1–42) altered the expression of various tight junction proteins in endothelial cells isolated from rat cerebral cortex microvessels, but again these effects were observed using a high concentration (20 μM) of Aβ (1–42) (Marco and Skaper 2006). Taking each of these parameters into account, it is not unexpected that the concentration of Aβ used in our model did not influence BBB permeability and underscores the validity of using this method to investigate Aβ exchange dynamics.

In order to properly evaluate the exchange of molecules across the BBB, an in vitro model must be able to discriminate transport-related phenomena from non-specific or paracellular movement. This

characteristic was evaluated using the permeability profiles of FD4 and fluorescein-Aβ, compounds of similar molecular weight (4kD). The dramatic difference in the movement of these two probes across the HBMEC (5-fold) illustrates the ability of this model to distinguish between the paracellular movement of FD4 and the facilitated transcytosis of Aβ. Our observation parallels the report by Strazielle et al. in which the basolateral-to-apical permeability of soluble iodinated Aβ was nearly 2.5 times greater than a paracellular marker of the same molecular weight (polyethylene glycol 4,000) across bovine brain endothelial cells (Strazielle et al. 2000).

It is well documented that Aβ crosses the BBB by a receptor-mediated form of endocytosis. The receptors primarily responsible for the transport of Aβ in the BBB are the low density lipoprotein receptor-related protein 1 (LRP1) and the receptor for advanced glycation end products (RAGE). These transporters play a major role in the movement of Aβ in and out of the central nervous system (CNS) and operate in opposing fashions with LRP1 transporting substrates from the brain to the blood, while RAGE transports in the blood-to-brain direction (Deane et al. 2004). Adequate expression and function of these transport systems is essential when examining Aβ interactions in the BBB. Western blot analysis revealed detectable levels of both LRP1 and RAGE in the HBMEC model. As for the functionality of these proteins, the HBMEC model responded to the presence of ligands for both proteins, as indicated by an altered transcytosis of fluorescein-Aβ (1–42). Furthermore, these alterations are consistent with observations reported in the literature. For LRP1, Yamada et al. observed the same degree of inhibition by RAP in a rat model of the BBB as we did in the HBMEC. Here, 500nM RAP reduced the internalization of iodinated Aβ in TR-BBB cells by 75% (Yamada et al. 2008). Similar results in human brain endothelial cells have been reported by Nazer et al. (2008). With respect to RAGE, we observed a significant modification in the transcytosis of fluorescein-Aβ (1–42) across the HBMEC in the presence of HMGB1, which resulted in an IC_{50} of around 0.1 μM. This value approaches the binding constant (Kd = 0.71 μM) recently reported for HMGB1 and RAGE (Liu et al. 2009). A demonstration of the flexibility of this model is borne out in the studies involving the RAGE antibody. The bi-directional transcytosis of fluorescein-Aβ (1–42) was examined following inhibition of RAGE via a monoclonal antibody. The impact of the antibody on fluorescein-Aβ (1–42) trancytosis across the membrane was dependent on the origin of the probe (i.e., apical or basolateral). Apical-to-basolateral trancytosis was hindered, while basolateral-to-apical trancytosis was enhanced by RAGE blockade. This effect is not unexpected due to the apical localization of RAGE in the BBB (Mackic et al. 1998). This aspect of the HBMEC model is essential in allowing one to investigate both the entry of molecules from the periphery into the brain and clearance from the brain to the blood. These examples provide additional evidence for the HBMEC as representative model of the BBB and offer credence for its use in examining Aβ transport in the BBB.

In addition to the need for a representative, easily maintained, in vitro model of the BBB, there is also a desire for a simple and rapid method of assessing Aβ transport phenomena in whole cells, as a majority of the assays currently used are tedious, costly, and time consuming. These assays often consist of components that are not commercially available and largely require the use of radioisotopes or more expensive, complex methods of detection such as multi-step immunoassays, liquid chromatography, or mass spectrometry. The transport studies performed in the current report used a fluorometric method comprised entirely of commercially available components. This approach offers a speed and simplicity that is lacking with many of the in vitro assays currently used, and may be useful as an initial assessment of Aβ transport in the BBB prior to the application of more advanced methodologies.

According to Gumbleton and Audus 2001, there are four general criteria an in vitro model must satisfy to appropriately assess permeability across the BBB: (1) a restrictive paracellular pathway, (2) a physiologically realistic architechture, i.e., cell lineage (endothelial vs. epithelial, brain vs. peripheral, capillary vs. arteriole/venuole), (3) functional expression of transporter mechanisms, and (4), ideally, ease of culture (Gumbleton and Audus 2001). We demonstrate that the in vitro BBB model in the current study adheres to each of these criteria. The HBMEC model poses a restrictive barrier comparable to existing models of the BBB, is of proper cell origin (i.e., human brain microvascular endothelial cells),

expresses functional, comparable, mechanisms of transport with respect to Aβ, and is easily maintained. Furthermore, we established the utility of the HBMEC model in examining Aβ exchange dynamics at the BBB and, in the process, offer a rapid method for examining Aβ transport in the BBB. As such, this method may be used to screen drugs that facilitate the clearance of Aβ across the BBB, opening the door to a new class of therapies for the treatment of AD.

Acknowledgments We would like to thank Diane and Robert Roskamp for their generosity in helping to make this work possible.

References

Artursson P (1990) Epithelial transport of drugs in cell culture. I: a model for studying the passive diffusion of drugs over intestinal absorptive (Caco-2) cells. J Pharm Sci 79: 476–482

Bowman GL, Kaye JA, Moore M, Waichunas D, Carlson NE, Quinn JF (2007) Blood-brain barrier impairment in Alzheimer disease: stability and functional significance. Neurology 68:1809–1814

Deane R, Wu Z, Zlokovic BV (2004) RAGE (yin) versus LRP (yang) balance regulates alzheimer amyloid beta-peptide clearance through transport across the blood-brain barrier. Stroke 35:2628–2631

Deli MA, Abraham CS, Kataoka Y, Niwa M (2005) Permeability studies on in vitro blood-brain barrier models: physiology, pathology, and pharmacology. Cell Mol Neurobiol 25:59–127

Eddy PE, Maleef BE, Hart TK, Smith PL (1997) In vitro models to predict blood-brain barrier permeability. Adv Drug Del Rev 23:185–198

Engelhardt B, Sorokin L (2009) The blood-brain and the blood-cerebrospinal fluid barriers: function and dysfunction. Semin Immunopathol 31:497–511

Gaillard PJ, de Boer AG (2000) Relationship between permeability status of the blood-brain barrier and in vitro permeability coefficient of a drug. Eur J Pharm Sci 12: 95–102

Giliberto L, Zhou D, Weldon R, Tamagno E, De Luca P, Tabaton M, D'Adamio L (2008) Evidence that the amyloid beta precursor protein-intracellular domain lowers the stress threshold of neurons and has a "regulated" transcriptional role. Mol Neurodegener 3:12

Gonzalez-Velasquez FJ, Kotarek JA, Moss MA (2008) Soluble aggregates of the amyloid-beta protein selectively stimulate permeability in human brain microvascular endothelial monolayers. J Neurochem 107:466–477

Guerin JL, Bobilya DJ (1997) Hypothalamic extract influences a blood-brain barrier model of porcine brain capillary endothelial cells. Neurochem Res 22:321–326

Gumbleton M, Audus KL (2001) Progress and limitations in the use of in vitro cell cultures to serve as a permeability screen for the blood-brain barrier. J Pharm Sci 90: 1681–1698

Jancso G, Domoki F, Santha P, Varga J, Fischer J, Orosz K, Penke B, Becskei A, Dux M, Toth L (1998) Beta-amyloid (1–42) peptide impairs blood-brain barrier function after intracarotid infusion in rats. Neurosci Lett 253:139–141

LaFerla FM, Green KN, Oddo S (2007) Intracellular amyloid-beta in Alzheimer's disease. Nat Rev Neurosci 8:499–509

Li G, Simon MJ, Cancel LM, Shi ZD, Ji X, Tarbell JM, Morrison B 3rd, Fu BM (2010) Permeability of endothelial and astrocyte cocultures: in vitro blood-brain barrier models for drug delivery studies. Ann Biomed Eng 38: 2499–2511

Liu R, Mori S, Wake H, Zhang J, Liu K, Izushi Y, Takahashi HK, Peng B, Nishibori M (2009) Establishment of in vitro binding assay of high mobility group box-1 and S100A12 to receptor for advanced glycation endproducts: heparin's effect on binding. Acta Med Okayama 63:203–211

Lue LF, Kuo YM, Roher AE, Brachova L, Shen Y, Sue L, Beach T, Kurth JH, Rydel RE, Rogers J (1999) Soluble amyloid beta peptide concentration as a predictor of synaptic change in Alzheimer's disease. Am J Pathol 155: 853–862

Ma SH, Lepak LA, Hussain RJ, Shain W, Shuler ML (2005) An endothelial and astrocyte co-culture model of the blood-brain barrier utilizing an ultra-thin, nanofabricated silicon nitride membrane. Lab Chip 5:74–85

Mackic JB, Stins M, McComb JG, Calero M, Ghiso J, Kim KS, Yan SD, Stern D, Schmidt AM, Frangione B, Zlokovic BV (1998) Human blood-brain barrier receptors for Alzheimer's amyloid-beta 1–40. Asymmetrical binding, endocytosis, and transcytosis at the apical side of brain microvascular endothelial cell monolayer. J Clin Invest 102:734–743

Marco S, Skaper SD (2006) Amyloid beta-peptide1–42 alters tight junction protein distribution and expression in brain microvessel endothelial cells. Neurosci Lett 401:219–224

Mehta PD (2007) Amyloid beta protein as a marker or risk factor of Alzheimer's disease. Curr Alzheimer Res 4: 359–363

Nagababu E, Usatyuk PV, Enika D, Natarajan V, Rifkind JM (2009) Vascular endothelial barrier dysfunction mediated by amyloid-beta proteins. J Alzheimers Dis 17:845–854

Nazer B, Hong S, Selkoe DJ (2008) LRP promotes endocytosis and degradation, but not transcytosis, of the amyloid-beta peptide in a blood-brain barrier in vitro model. Neurobiol Dis 30:94–102

Skoog I, Wallin A, Fredman P, Hesse C, Aevarsson O, Karlsson I, Gottfries CG, Blennow K (1998) A population study on blood-brain barrier function in 85-year-olds: relation to Alzheimer's disease and vascular dementia. Neurology 50:966–971

Strazielle N, Ghersi-Egea JF, Ghiso J, Dehouck MP, Frangione B, Patlak C, Fenstermacher J, Gorevic P (2000) In vitro evidence that beta-amyloid peptide 1–40 diffuses across the blood-brain barrier and affects its permeability. J Neuropathol Exp Neurol 59:29–38

Terasaki T, Hosoya K (2001) Conditionally immortalized cell lines as a new in vitro model for the study of barrier functions. Biol Pharm Bull 24:111–118

Ujiie M, Dickstein DL, Carlow DA, Jefferies WA (2003) Blood-brain barrier permeability precedes senile plaque formation in an Alzheimer disease model. Microcirculation 10:463–470

Yamada K, Hashimoto T, Yabuki C, Nagae Y, Tachikawa M, Strickland DK, Liu Q, Bu G, Basak JM, Holtzman DM, Ohtsuki S, Terasaki T, Iwatsubo T (2008) The low density lipoprotein receptor-related protein 1 mediates uptake of amyloid beta peptides in an in vitro model of the blood-brain barrier cells. J Biol Chem 283:34554–34562

Zipser BD, Johanson CE, Gonzalez L, Berzin TM, Tavares R, Hulette CM, Vitek MP, Hovanesian V, Stopa EG (2007) Microvascular injury and blood-brain barrier leakage in Alzheimer's disease. Neurobiol Aging 28:977–986